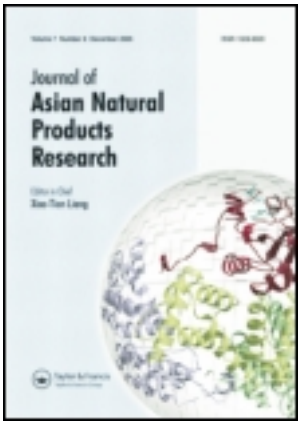

Journal of Asian Natural Products Research

Publication details, including instructions for authors and subscription information:
http://www.tandfonline.com/loi/ganp20

Synthesis, anticancer, and antibacterial activities of piplartine derivatives on cell cycle regulation and growth inhibition

J. Ujwal Kumar [a], G. Shankaraiah [b], R. Sateesh Chandra Kumar [b], V. V. Pitke [a], G. Tirupathi Rao [a], B. Poornima [b], K. Suresh Babu [b] & A.S. Sreedhar [a]

[a] Centre for Cellular and Molecular Biology, Hyderabad, 500 007, India

[b] Division of Organic Chemistry-I, Natural Products Laboratory, Indian Institute of Chemical Technology, Hyderabad, 500 007, India

Published online: 13 May 2013.

To cite this article: J. Ujwal Kumar, G. Shankaraiah, R. Sateesh Chandra Kumar, V. V. Pitke, G. Tirupathi Rao, B. Poornima, K. Suresh Babu & A.S. Sreedhar (2013): Synthesis, anticancer, and antibacterial activities of piplartine derivatives on cell cycle regulation and growth inhibition, Journal of Asian Natural Products Research, 15:6, 658-669

To link to this article: http://dx.doi.org/10.1080/10286020.2013.769965

Journal of Asian Natural Products Research, 2013
Vol. 15, No. 6, 658–669, http://dx.doi.org/10.1080/10286020.2013.769965

Synthesis, anticancer, and antibacterial activities of piplartine derivatives on cell cycle regulation and growth inhibition

J. Ujwal Kumar[a], G. Shankaraiah[b], R. Sateesh Chandra Kumar[b], V. V. Pitke[a], G. Tirupathi Rao[a], B. Poornima[b], K. Suresh Babu[b]* and A.S. Sreedhar[a]*

[a]*Centre for Cellular and Molecular Biology, Hyderabad 500 007, India;* [b]*Division of Organic Chemistry-I, Natural Products Laboratory, Indian Institute of Chemical Technology, Hyderabad 500 007, India*

(*Received 29 October 2012; final version received 21 January 2013*)

A series of piplartine derivatives were synthesized via Baylis–Hillman reaction and evaluated for anticancer and antibacterial activities. The cytotoxicity of these compounds was examined in two different human tumor cell lines, IMR-32 and HeLa. The antibacterial activity was examined in *Staphylococcus aureus* and *Pseudomonas aeruginosa*. The results showed that compounds **2b**, **2e**, and **2j** were found to be the most active compounds, which displayed line no cytotoxicity, but G2–M cell cycle arrest in tumor cells, and showed cytostatic effects in bacteria.

Keywords: *Piper chaba*; piplartine; piplartine derivatives; anticancer activity; antibacterial activity

1. Introduction

Cancer is one of the most serious threats against human health in the world [1]. Over the past few decades, extensive research has led to the development of a plethora of chemotherapeutic agents [2,3]. The limitations of current anticancer drugs and rapid development of drug resistance [4–6] have highlighted the need for the discovery of new anticancer agents, preferably with novel mechanisms of action. To identify new chemical entities for a more effective treatment of cancer, drug designers can follow many strategies, but the crucial decision is always the selection of a suitable starting point from the vast chemical space [7].

In this respect, natural products evolved as privileged structures [8] and biologically prevalidated leads; in other words, as molecules that have probably evolved evolutionarily to exert highly specialized functions. About 74% of anticancer compounds are from both natural and natural product-derived products, indicating potency of these scaffolds [2,3]. The unprecedented structures of these molecules make them excellent synthetic targets, and their potent activity against a broad number of therapeutic indications makes these natural products as excellent drug lead candidates for new therapeutics. *Piper* species (Piperaceae) are important plants in traditional medicine [9]. The alkaloid–amide components isolated from *Piper* species show varied cellular effects such as anti-inflammatory, anticancer, and cytotoxic effects, however, through unidentified cellular mechanism [10,11]. In connection with recent investigations of *Piper* species for value-added products [12,13], we have isolated large quantities of piplartine (**1**) (2%) from *Piper chaba*, which prompted us to synthesize derivatives and screen the anticancer activity.

*Corresponding authors. Email: suresh@iict.res.in; assr@ccmb.res.in

In this study, several derivatives of piplartine were synthesized by Baylis–Hillman reaction and examined for anticancer activity using human neuroblastoma and cervical cancer cell lines and for antibacterial activity using *Staphylococcus aureus* and *Pseudomonas aeruginosa*. The rationale to study both anticancer and antibacterial activities with two different cells and bacteria was to examine the unique feature of piplartine for cytostatic property.

2. Results and discussion

The basic skeleton of piplartine consists of trimethoxycinnamyl moiety, attached to six-membered piperidone moiety that contains double bond at the third position. This study aimed to explain structure–activity relationship studies on piperidone moiety by introducing several aromatic rings using Baylis–Hillman reaction with various aldehydes. Thus, the target compounds **2a**–**2j** were prepared through one-step reaction of piplartine with various aldehydes using 1,4-diazabicyclo[2.2.2]octane (DABCO) in a catalytic amount at room temperature in 1,4-dioxane (Scheme 1).

3. Biological activity

3.1 Anticancer activity

The anticancer activity of piplartine derivatives was examined in IMR-32 and HeLa cancer cells. Tumor cells (1×10^6/ml) were treated with varying concentrations of piplartine derivatives (**2a**–**2j**) ranging from 2, 4, 8, 12, to 24 μM for 18 h, and analyzed by 3-(4,5-dimethylthiazol-2-yl)-2,5-diphenyltetrazolium bromide (MTT) assay. We have not included the parental compound piplartine since its biological activity has been reported in IMR-32 and HeLa cells [13]. None of the compounds were found to be cytotoxic from the MTT assay. Increasing drug concentrations also had no effect in inducing the cytotoxicity (data not presented). Our previous studies with piplartine indicated that piplartine alone is not cytotoxic, but exhibits cytostatic property and accumulates cells in G1–S cell cycle transition [13]. Therefore, to assess the cell cycle inhibition of piplartine derivatives, tumor cells after respective drug treatments were subjected to the fluorescence-activated cell sorting (FACS) analysis. Among all the derivatives, in contrast to the parental compound piplartine that induced G1–S arrest [13], compounds **2b**, **2e**, and **2j** showed significant G2–M accumulation of cells in both HeLa (Figure 1(a)) and IMR-32 cells (Figure 1(b)).

The current approach of drug discovery to combat cancer suggests that combinatorial treatments are rather beneficial for effective cell killing [14]. Therefore,

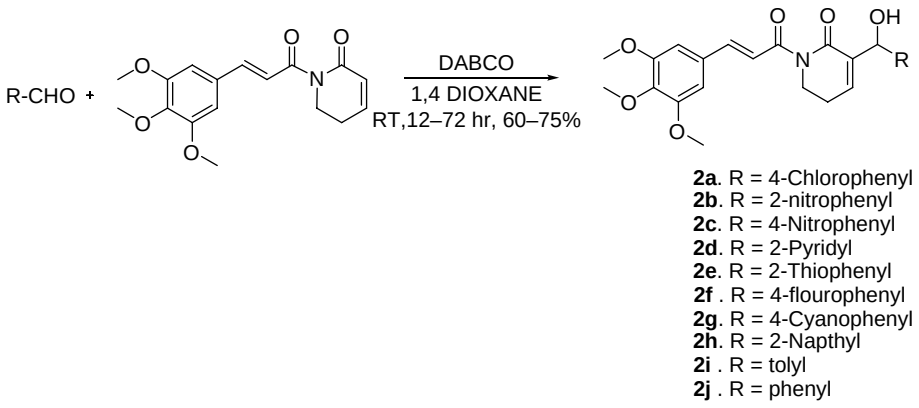

Scheme 1. Synthesis of piplartine derivatives.

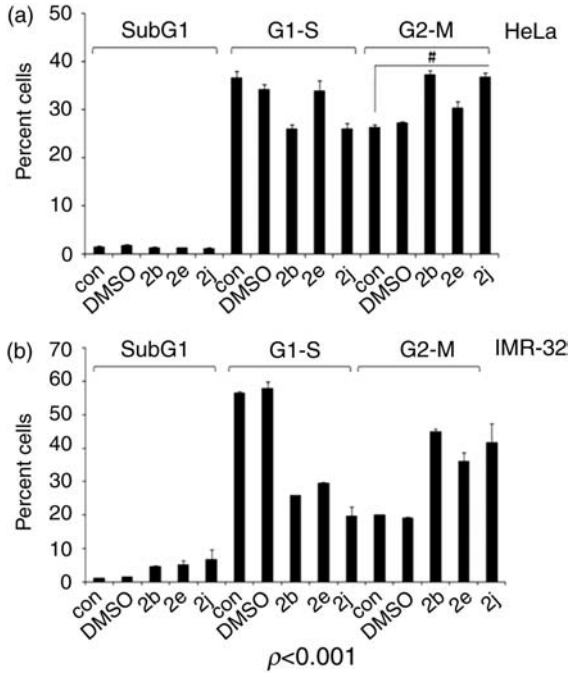

Figure 1. Effect of piplartine derivatives on cell cycle regulation was analyzed by FACS. (a) HeLa and (b) IMR-32 cells were treated with compounds **2b**, **2e**, and **2j** and analyzed in fluorescence-activated cell sorter. DMSO was used as a solvent control.

we have selected two chemotherapeutic drugs curcumin and cisplatin to use in combination with piplartine derivatives in human cervical cancer cells, HeLa. Curcumin was shown to be non-cytotoxic at 15 μM concentrations in IMR-32 when used in combination with piplartine [13]; hence, HeLa cells alone were used to examine the combination drug effects. Another chemotherapeutic drug, cisplatin, induces DNA damage and apoptosis at higher concentrations, but at lower doses it is found to be ineffective [15]. Therefore, in this study, we have used 1 μM cisplatin in combination with piplartine derivatives **2b**, **2e**, and **2j**. Interestingly, both curcumin (Figure 2(a) and cisplatin combination with piplartine derivatives, **2b**, **2e**, and **2j**).

The results obtained from Figure 1 (a),(b) strongly suggested cell cycle-specific inhibition of piplartine derivatives **2b**, **2e**, and **2j**. It is increasingly apparent that the cell cycle plays a critical role in chemosensitizing the combination chemotherapy. Chemotherapeutic drug, hydroxyurea (HU), belongs to the class of anti-metabolite drugs that inhibit cell growth. Low concentrations of HU synchronize tumor cells in G1–S phase transition [16]. Colcemid is a less toxic derivative of colchicine, a chemotherapeutic drug, that inhibits microtubule polymerization and arrests cells in metaphase (G2–M transition) due to interference of the drug with spindle formation [17]. To corroborate piplartine-induced G2–M-specific cell cycle block, IMR-32 and HeLa tumor cells were treated with derivatives of piplartine in combination with low doses of HU and colcemid. Interestingly, in the individual drug treatments, HU- and colcemid-induced G1–S and G2–M transition, respectively, while the combination drug treatments retained cells in HU-induced G1–S phase (Figure 3(a),(b)) or colcemid-induced

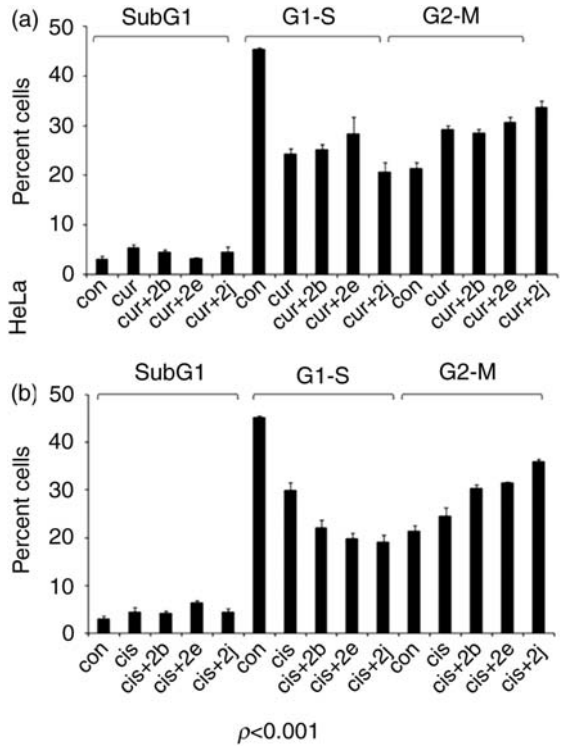

Figure 2. Effect of piplartine derivatives in combination treatment with anticancer agents was examined by FACS analysis. (a) HeLa cells treated with compounds **2b**, **2e**, and **2j** in combination with curcumin were examined. (b) IMR-32 cells treated with compounds **2b**, **2e**, and **2j** in combination with DNA damaging agent cisplatin were examined.

G2–M phase (Figure 3(c),(d)). Protein kinases are identified as signatures of cancer [18–20]. The mitogen-activated protein kinase (MAPK) family of kinases connects extracellular stimuli with diverse cellular responses. Although the MAPK family has been studied extensively, the role of these kinases in cell growth and cell cycle control has become increasingly complex [21]. Therefore, we have examined the activation of MAPK members ERK1/2 in our drug combinations. Though there was a difference in ERK1/2 basal levels, the enhanced ERK1/2 activation was predominant in all the piplartine treatments when used alone or in combination treatments (Figure 4(a)–(c)). Although enhanced and sustained MAPK activity in our treatments is surprising despite the growth arrest, Pumiglia and Decker [22] provided the information that sustained MAP kinase activity can also lead to the inhibition of CDK activity and growth arrest to support our observations.

The cell cycle is driven by a family of proteins called cyclin-dependent kinases (CDKs) [23]. Since protein kinases are identified as signatures of cancer and piplartine derivatives show selective cell cycle inhibition, we have analyzed CDK1, CDK2, and CDK6 both alone and in combination drug treatments. The derivatives **2b**, **2e**, and **2j** showed a decrease in CDK6 (a kinase that is involved in G1 entry of cell cycle) expression in both the cell types (Figure 4(a)). In IMR-32 cells, HU combination showed a decrease in CDK6, and in HeLa cells, HU combination showed an increase in CDK6. In IMR-32 cells, colcemid combination showed a decrease in CDK6, and in HeLa cells,

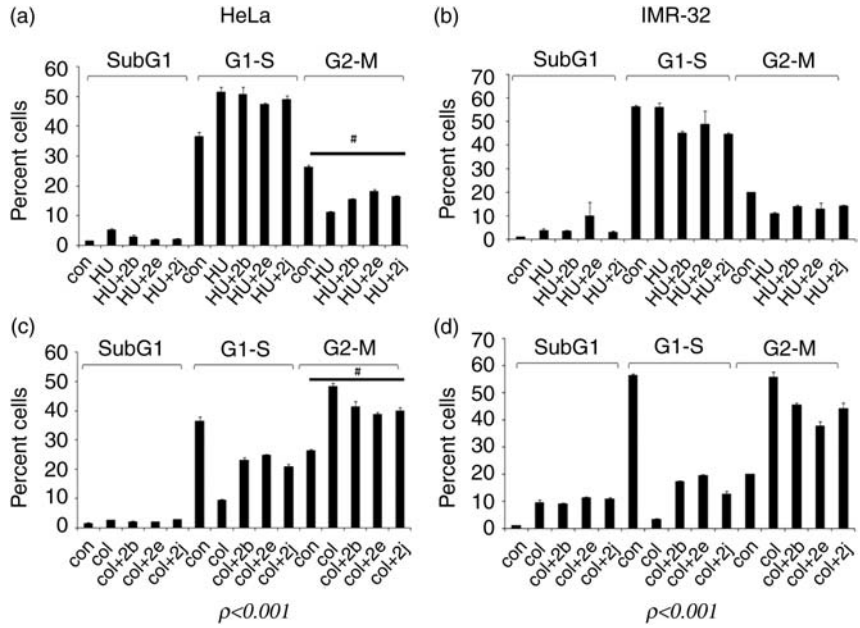

Figure 3. Effect of piplartine derivatives on synchronization of cells to reversible cytostatic drugs was examined by FACS analysis. (a) and (c) HeLa cells treated with compounds **2b**, **2e**, and **2j** after respective treatments with HU or colcemid (Col), respectively. (b) and (d): IMR-32 cells were treated with compounds **2b**, **2e**, and **2j** after respective treatments with HU or Col, respectively.

colcemid combination showed an increase in CDK6 (Figure 2(b),(c)). The G1–S kinase CDK2 levels were unaffected, but the G2–M kinase CDK1 levels were decreased by the treatment in both the cells. There was an increase in CDK1 and CDK2 levels in HU combination in both IMR-32 and HeLa cells, whereas colcemid combination showed a drastic decrease in CDK2 expression levels (Figure 4(b),(c)).

Since compounds **2b**, **2e**, and **2j** showed significant G2–M cell cycle inhibition without cell death, we examined alterations in cell morphology. All the three compounds showed a change in cell morphology from well-spread adhesion to elongation, followed by leaving the substratum in both HeLa and IMR-32 cells. In the combination treatments with colcemid and HU, we observed enhanced elongation and inhibition of cell adhesion in both the cells (Figure 5(a),(b)).

3.2 Antibacterial activity

Medicinal plants also represent a rich source of antimicrobial agents; thus, interest has revived recently in the investigation of medicinal plants to identify novel active phytochemicals that might lead to new classes of microbial drug development. In order to examine the antibacterial activity of piplartine and its derivatives, we treated *S. aureus* and *P. aeruginosa* a gram-negative and a gram-positive bacteria, respectively, with piplartine and derivatives at a final concentration of 48 μM. Interestingly, some of the derivatives exhibited significant antibacterial activity, however, with varied strengths. Derivatives **2b**, **2e**, and **2j** showed a significant growth inhibition of 7%, 16%, and 22% ($p < 0.05$, $p < 0.01$, and $p < 0.01$), respectively, at 48 μM concentration treatment in *P. aeruginosa*. The parental compound, piplartine, induced 13.7% growth inhibition ($p < 0.001$) in

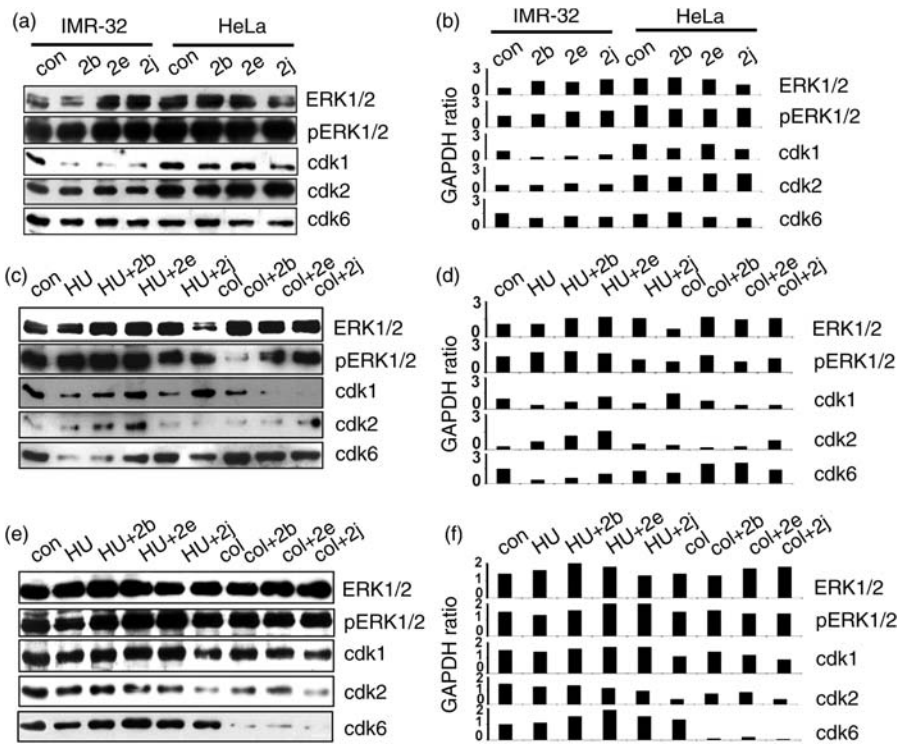

Figure 4. Immunoblot analysis of tumor cells treated with piplartine derivatives. (a) HeLa and IMR-32 cells treated with **2b**, **2e**, and **2j** compounds analyzed for both non-phospho and phosphorylated ERK1/2, CDK1, CDK2, and CDK6. (b) Densitometry analysis of 'A' protein expression versus GAPDH. (c) HeLa cells treated with HU and colcemid combinations with piplartine derivatives **2b**, **2e**, and **2j**. (d) Densitometry analysis of 'C' protein expression versus GAPDH. (e) IMR-32 cells treated with HU and colcemid combinations with piplartine derivatives **2b**, **2e**, and **2j**. (f) Densitometry analysis of 'E' protein expression versus GAPDH.

P. aeruginosa (Figure 6(a)). Derivatives **2c**, **2e**, **2f**, **2i**, and **2j** showed significant growth inhibition of 10.7%, 19.7%, 20.9%, 39.4%, and 33.6% ($p < 0.01$, $p < 0.01$, $p < 0.01$, $p < 0.001\%$, and $p < 0.001$), respectively at 48 μM concentration treatment in *S. aureus*. The parental compound, piplartine, induced 14.7% growth inhibition ($p < 0.01$) in *P. aeruginosa* (Figure 6(b)). Although the growth showed differential response, all the derivatives significantly interfered with bacterial proliferation suggesting the potential antibacterial activity of piplartine derivatives.

4. Conclusion

In conclusion, we show that among 10 piplartine derivatives, 2-nitrophenyl (**2b**), thiophenyl (**2e**), and phenyl (**2j**) derivatives showed significant cytostatic activity against different cancer cells. The derivatives **2b**, **2e**, and **2j** showed enhanced mitogen signal activation that leads to enforced cell cycle inhibition arresting cells in G2–M phase of the cell cycle. Further cell cycle entry has been compromised by the combination drug treatment with HU- and colcemid-inhibiting CDK6. The derivatives also showed antibacterial activity, however, with varied specificity against gram-positive and gram-negative bacteria.

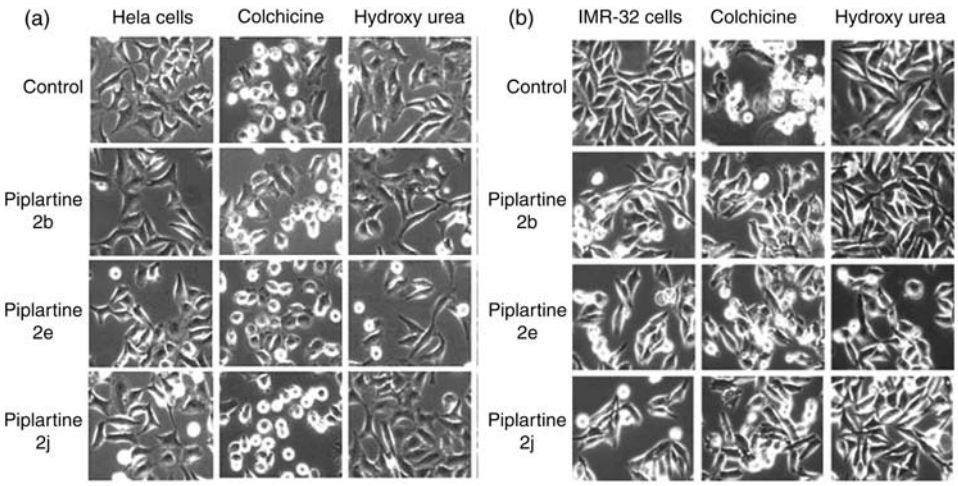

Figure 5. Morphological analysis of drugs-treated tumor cells. (a) HeLa, (b) IMR-32 cells after respective treatments.

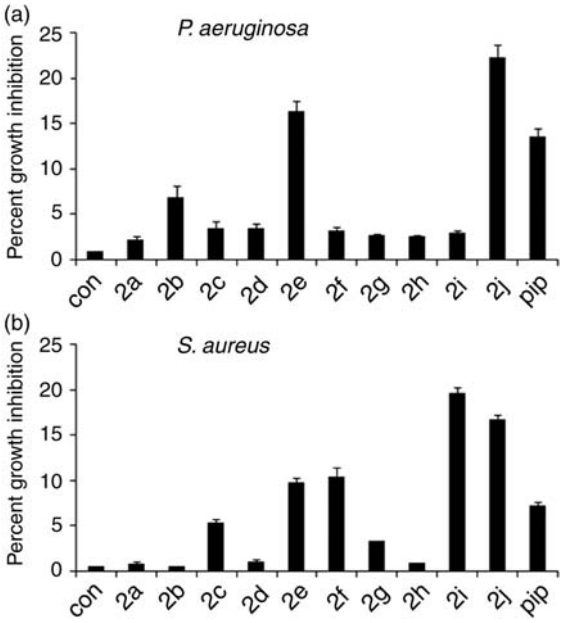

Figure 6. Evaluation of piplartine derivatives on bacterial growth. The effect of piplartine derivatives **2b**, **2e**, and **2j** was studied in *P. aeruginosa* (a) and *S. aureus* (b). *Con*, control cells; *pip*, parental piplartine compound.

5. Experimental

5.1 General experimental procedures

Melting points were recorded on a Fisher scientific melting point apparatus (Pittsburgh, PA, USA) and are uncorrected. The ^{1}H and ^{13}C NMR spectra were recorded on a Bruker FT-300 MHz spectrometer (Bruker, Fallanden, Switzerland) at 300 MHz for ^{1}H and 75 MHz for ^{13}C, respectively, using trimethylsilane (TMS) as internal standard. The chemical shifts are expressed as (δ) values in

parts per million (ppm), and the coupling constants (*J*) are given in hertz (Hz). Spin multiplicities are described as s (singlet), brs (broad singlet), d (doublet), t (triplet), q (quartet), and m (multiplet). Mass spectra were measured on LC-MSD-Trap-SL instrument (Agilent, Santa Clara, CA, USA). The solvents were purified by distillation under nitrogen from the indicating drying agent, and freshly prepared dichloromethane (calcium hydride) and acetone (potassium permanganate) were used. Column chromatography was carried out using silica gel 100–200 mesh (Acme Silica gel, Mumbai, India), and precoated silica gel plates (Merck, 60 F254, Darmstadt, Germany) were used for preparative thin-layer chromatography (TLC). Chemicals and reagents were purchased from Sigma-aldrich Chemical Co., Bengaluru, India. Other chemicals of analytical grade were procured from indigenous manufacturers (Rankem, New Delhi, India).

5.2 Extraction and isolation of piplartine from Piper chaba

The roots of the plant *P. chaba* were procured from Indian Medicines and Pharmaceuticals Limited (IMPCL), Uttarakhand, India. It was authenticated by Dr K. Madhava Chetty, and a voucher specimen has been deposited in the herbarium of the Botany Department, Sri Venkateswara University, Tirupati, Andhra Pradesh, India. The roots of *P. chaba* (5 kg) were shade dried, powdered, and extracted with hexane in a Soxhlet apparatus at 60°C temperature for 48 h. The resulting hexane extract was filtered to yield the yellow colored piplartine (2 g).

5.3 Cell culture and drugs treatment

HeLa and human neuroblastoma (IMR-32) tumor cells were maintained in Dulbecco's Modified Eagle's Medium containing 10% fetal calf serum, penicillin (100 U/ml), and streptomycin (50 μg/ml) in a humidified incubator chamber (37°C) supplied with 5% CO_2. Exponentially growing tumor cells (1×10^6/ml) in the complete medium were treated with 24 μM concentrations of piplartine derivatives, 15 μM curcumin, 2 μM paclitaxel (Sigma Aldrich, St Louis, MI, USA), 2 μM HU, colcemid, and cisplatin (Calbiochem, Billerica, MA, USA) either alone or in combination. For primary screening to assess the dose-dependent studies, we used 2, 4, 8, 12, and 24 μM concentrations of piplartine. The treatment continued for 20 h for HeLa cells and 36 h for IMR-32 cells at 37°C, and after respective drug treatments, cells were harvested for subsequent experiments. The difference in incubation time was decided based on doubling time of each tumor type and the type of experiment, either cytotoxicity or cell cycle analysis.

5.4 The morphological analysis using ApoTome microscope

Cells grown on cover glass (Thermo Fisher Scientifics, 22 × 22 mm) and treated with piplartine derivative either alone or in combination with known anticancer agents for 20 or 36 h time intervals were visualized using inverted microscope (Axiovert 200, 20 × magnifications).

5.5 The cell viability, cell cycle, and cell death analysis

The cell viability was determined by trypan blue exclusion assay before processing the cells for further experiments. Control- and drugs-treated tumor cells were washed with phosphate-buffered saline, stained with 50 μg/ml propidium iodide (containing 0.1% triton X-100 and 22 μg/ml RNase). Cells were either visualized under a fluorescence microscope (Nikon) or analyzed in a fluorescence-activated cell sorter (FACS Calibur, BD, Beckton Dickinson). The 'sub-G1 peak' represents dead cells, cells with single chromosome set (2N) are represented as G1–S population, and cells

with double chromosome set (4N) are represented as G2–M population.

5.6 SDS-Polyacrylamide gel electrophoresis and Western blot analysis

Tumor cells after respective drug treatments were lyzed with 50 mM Tris lysis buffer, pH 7.4 (150 mM NaCl, 5 mM EDTA, 0.1% NP-40, 1MM PMSF, 1X protease inhibitor cocktail; 60 min, 4°C). Protein concentrations of cell lysates were estimated by Bradford method (Bradford 1976), using bovine serum albumin as standard. Twenty micrograms of total cell lysate were mixed with Laemmli buffer containing 100 μl dithiothreitol, boiled for five minutes, and the samples were subjected to 10% sodium dodecyl sulfate-polyacrylamide gel electrophoresis (SDS-PAGE). Proteins were transferred from the gel to nitro-cellulose membrane using a semidry protein gel transfer apparatus (Amersham Biosceinces, PA, USA). Transfer of proteins was confirmed by Ponceau-S staining, and the blot was processed for Western blot analysis. Blocking of the membrane was done with 5% skimmed milk powder and 0.1% Tween 20 in 1X TBE (89 mM Tris/89 mM borate/2 mM ethylenediaminetetraacetic acid) buffer, and incubation was done with appropriate primary antibody followed by a horseradish peroxidase-conjugated secondary antibody at room temperature. Labeled bands were visualized using BM-Chemiluminescence kit (Roche, Basel, Switzerland). The antibodies for ERK1/2 and pERK1/2 (1:1000 dilution), CDK1 (1:1000), CDK2 (1:1000), and CDK6 (1:1000) were obtained from Santa Cruz Biosciences (Santa Cruz, CA, USA).

5.7 Bacterial growth conditions and treatments

Bacteria (*S. aureus* and *P.* aeruginosa) were grown in Luria Bertani (LB) medium. Briefly, in each experiment, a single-bacterial colony was inoculated into 2 ml LB broth, grown over night at 37°C, 200 rpm shaking. In the next day, fresh culture was inoculated from overnight culture (1:100 dilution), allowed to grow for 3 h, to obtain maximum cells in mid-log phase of growth. Using different drug concentrations ranging from 2, 4, 6, 12, 24, 48, to 96 μM, the optimal concentration was calculated from at least 50% bacterial growth of at least one of the drugs tested in this study. A concentration above 48 μM was found to be ineffective and failed to show any additional affects on bacterial growth. Piplartine derivatives were added to these cultures at a final concentration of 48 μM, incubated for overnight (18 h) at appropriate growth conditions for further analysis. Control cells were maintained without treatment, whereas solvent control was maintained treating cells only with dimethylsulfoxide (DMSO).

5.8 Analysis of cytotoxicity by spectrometric measurements

After 18 h of treatment with appropriate natural compound fraction, one milliliter bacterial culture was taken in 1.5 ml disposable sterile plastic cuvette, and the optical density was measured at 600 nm using the spectrophotometer (Shimadzu double-beam spectrophotometer, Model 1601). The DMSO-treated cells were used for normalization. The optical density values obtained were converted to percent cytotoxicity and plotted on a bar diagram. Each experiment was repeated at least three times, and standard error was marked on each bar value.

5.9 Statistical analysis of data

Data in the bar diagrams are reported as mean ± SD. The control groups were compared with drug-treated groups, and the significance values were calculated by paired Student's *t*-test. Data represented is an average of three independent experiments in each group. The *P* values

represented are ***$p < 0.001$, **$p < 0.01$, and *$p < 0.05$.

6. General procedure for the synthesis of piplartine derivatives (2a–j)

To a solution of aldehyde (0.62 mM) and piplartine in 1,4-dioxane was added DABCO in catalytic amount and stirred for 12–72 h at room temperature. The reaction progress was monitored by TLC. After completion, reaction mixture was partitioned between *t*-butyl methyl ether (5 ml) and water (10 ml). The organic phase was washed with brine, dried over anhydrous Na_2SO_4, filtered, and evaporated under reduced pressure to give the crude product, which was purified by flash column chromatography to yield the pure compounds.

6.1 Spectroscopic data of conjugates (2a-2j)

*6.1.1 (E)-3-((4-Chlorophenyl)(hydroxy) methyl)-1-(3-(3,4,5-trimethoxyphenyl) acryloyl)-5,6-dihydropyridin-2(1H)-one (**2a**)*

Yield 60%; yellow oil; ^{1}H NMR (300 MHz, $CDCl_3$): δ 7.64–7.54 (1H, d, $J = 15.4$ Hz), 7.33–7.23 (5H, m), 6.76 (3H, m), 5.62 (1H, s), 3.96 (2H, t, $J = 7.5$ Hz), 3.90 (6H, s), 3.83 (3H, s), 2.41 (2H, m).^{13}C NMR (75 MHz, $CDCl_3$): δ ^{13}C NMR (75 MHz, $CDCl_3$): δ 168.3, 166.1, 153.4 (2C), 144.2, 140.9 (2C), 139.9, 138.1, 133.5, 130.4, 128.5 (2C), 128.0 (2C), 120.8, 105.7 (2C), 71.4, 60.7, 56.0 (2C), 41.5, 24.5; ESI-MS: *m/z* 457 $[M]^+$, HR-ESI-MS: *m/z* 480.1139 $[M + Na]^+$ (calcd for $C_{24}H_{24}NO_6ClNa$, 480.1190).

*6.1.2 (E)-3-(Hydroxy(4-nitrophenyl)methyl)-1-(3-(3,4,5-trimethoxyphenyl)acryloyl)-5,6-dihydropyridin-2(1H)-one (**2b**)*

Yield 65%; pale yellow solid, mp 137°C; ^{1}H NMR (300 MHz, $CDCl_3$): δ 7.93 (1H, d, $J = 9.0$ Hz), 7.87 (1H, d, $J = 7.7$ Hz), 7.72 (2H, m), 7.50 (1H, m), 7.37 (1H, d, $J = 15.6$ Hz) 6.78 (2H, s), 6.59 (1H, t, $J = 8.1$ Hz), 6.27 (1H, br s), 3.98 (2H, m), 3.92 (6H, s), 3.87 (3H, s), 2.45 (2H, m). ^{13}C NMR (75 MHz, $CDCl_3$): δ 168.3, 166.2, 160.6, 153.3 (2C), 144.2, 140.7, 140.4, 138.4, 137.1, 130.4, 128.3, 128.2, 120.8, 115.3, 115.1, 105.7 (2C), 71.4, 60.6, 56.0 (2C), 41.5, 24.5; ESI-MS: *m/z* 469 $[M + H]^+$; HR-ESI-MS: *m/z* 469.1628 $[M + H]^+$ (calcd for $C_{24}H_{25}N_2O_8$, 469.1610).

*6.1.3 (E)-3-(Hydroxy(4-nitrophenyl)methyl)-1-(3-(3,4,5-trimethoxyphenyl)acryloyl)-5,6-dihydropyridin-2(1H)-one (**2c**)*

Yield 63%; yellow solid, mp 135°C; ^{1}HNMR (300 MHz, $CDCl_3$): δ 8.20 (2H, d, $J = 8.6$ Hz), 7.63 (1H, d, $J = 15.6$ Hz), 7.60 (2H, d, $J = 8.8$ Hz), 7.28 (1H, d, $J = 15.6$ Hz), 6.73 (3H, m), 5.71 (1H, br s), 4.01 (2H, m), 3.91 (6H, s), 3.86 (3H, s), 2.50 (2H, m).^{13}C NMR (75 MHz, $CDCl_3$): δ 168.0, 165.7, 153.0 (2C), 148.1, 147.1, 144.2, 141.5 (2C), 136.9, 129.9, 126.9 (2C), 123.2 (2C), 120.2, 105.3 (2C), 71.4, 60.4, 55.7 (2C), 41.2, 24.1; ESI-MS: *m/z* 469 $[M + H]^+$; HR-ESI-MS: *m/z* 469.1628 $[M + H]^+$ (calcd for $C_{24}H_{24}N_2O_8$, 469.1610).

*6.1.4 (E)-3-(Hydroxy(pyridin-2-yl) methyl)-1-(3-(3,4,5-trimethoxyphenyl) acryloyl)-5,6-dihydropyridin-2 1H)-one (**2d**)*

Yield 58%; oil; ^{1}H NMR (300 MHz, $CDCl_3$): δ 8.49 (1H, $J = 4.7$ Hz) 7.70–7.53 (3H, m), 7.33 (1H, d, $J = 15.4$ Hz), 7.20(1H, t, $J = 11.7$ Hz), 7.02 (1H, t, $J = 7.3$ Hz), 6.74 (2H, s), 5.72 (1H, s), 4.10 (2H, m), 3.91 (6H, s), 3.85 (3H, s), 2.51 (2H, m).^{13}C NMR (75 MHz, $CDCl_3$): δ 168.4, 166.1, 160.2, 153.4 (2C), 148.1, 143.9, 141.1, 137.7, 136.8 (2C), 130.6, 122.5, 121.7, 121.1, 105.7 (2C), 70.5, 60.7, 55.8 (2C), 41.6, 24.6; ESI-MS: *m/z* 425 $[M + H]^+$.

*6.1.5 (E)-3-(Hydroxy(thiophen-2-yl) methyl)-1-(3-(3,4,5-trimethoxyphenyl) acryloyl)-5,6-dihydropyridin-2(1H)-one (**2e**)*

Yield 58%; yellow oil; ^{1}H NMR (300 MHz, $CDCl_3$): δ 7.60 (1H, d, $J = 15.4$ Hz), 7.33 (1H, d, $J = 15.4$ Hz), 7.21 (1H, dd, $J = 4.9$ Hz, $J = 1.1$ Hz), 6.94 (2H, m), 6.84 (1H, t, $J = 7.9$ Hz), 6.74 (2H, s), 5.83 (1H, s), 4.01 (2H, m), 3.89 (6H, s), 3.82 (3H, s), 2.51 (2H, m). ^{13}C NMR (75 MHz, $CDCl_3$): δ 168.4, 165.9, 153.4 (2C), 146.0, 144.0, 140.9 (2C), 137.2, 130.4, 136.9, 125.5 (2C), 120.9, 105.6 (2C), 71.0, 60.9, 56.7 (2C), 41.4, 24.0; ESI-MS: *m/z* 429 $[M]^+$; HR-MS (ESI): *m/z* 452.1143 $[M + Na]^+$ (calcd for $C_{22}H_{23}NO_6SNa$, 452.1138).

*6.1.6 (E)-3-((4-Fluorophenyl)(hydroxy) methyl)-1-(3-(3,4,5-trimethoxyphenyl) acryloyl)-5,6-dihydropyridin-2(1H)-one (**2f**)*

Yield 55%; pale yellow oil; ^{1}H NMR (300 MHz,$CDCl_3$): δ 7.59 (1H, d, $J = 15.4$ Hz), 7.32 (3H, m), 7.01 (2H, m), 6.72 (2H, s), 6.67 (1H, t, $J = 7.7$ Hz), 5.60 (1H, s), 3.94 (2H, m), 3.89 (6H, s), 3.84 (3H, s), 2.48 (2H, m). ^{13}C NMR (75 MHz, $CDCl_3$): δ 168.3, 166.2, 160.6, 153.4 (2C), 144.2, 140.7, 140.4, 138.4, 137.1, 130.4, 128.3, 128.2, 120.8, 115.3, 115.1, 106.5 (2C), 71.6, 60.8, 56.0 (2C), 41.5, 24.5; ESI-MS: *m/z* 442 $[M + H]^+$; HR-ESI-MS: *m/z* 464.1492 $[M + Na]^+$ (calcd for $C_{24}H_{24}NO_6FNa$, 464.1485).

*6.1.7 (E)-4-(Hydroxy(2-oxo-1-(3-(3,4,5-trimethoxyphenyl)acryloyl)-1,2,5,6-tetrahydropyridin-3-yl) methyl)benzonitrile (**2g**)*

Yield 60%; pale yellow oil; ^{1}H NMR (300 MHz, $CDCl_3$): δ 7.59–7.43 (5H, m), 7.23 (1H, d, $J = 15.4$ Hz), 6.74 (1H, m), 6.72 (2H, s), 5.64 (1H, s), 3.89 (2H, m), 3.87 (6H, s), 3.83 (3H, s), 2.45 (2H, m). ^{13}C NMR (75 MHz, $CDCl_3$): δ 168.2, 165.6, 153.2 (2C), 147.2, 144.0, 141.3 (2C), 137.5, 131.8 (2C), 130.2, 127.2 (2C), 120.7, 118.2, 111.3, 105.6 (2C), 70.8, 60.5, 55.9 (2C), 41.4, 24.3; ESI-MS: *m/z* 471 $[M + Na]^+$, HR-ESI-MS: *m/z* 471.1538 $[M + Na]^+$ (calcd for $C_{25}H_{24}N_2O_6Na$, 471.1532).

*6.1.8 (E)-3-(Hydroxy(naphthalen-2-yl) methyl)-1-(3-(3,4,5-trimethoxyphenyl) acryloyl)-5,6-dihydropyridin-2(1H)-one (**2h**)*

Yield 63%; pale brown solid, mp 143°C; ^{1}H NMR (300 MHz, $CDCl_3$): δ 7.84 (1H, s), 7.86 (3H, m), 7.58 (1H, d, $J = 15.4$ Hz), 7.42 (3H, m), 7.32(1H, d, $J = 15.4$ Hz), 6.73 (2H, s), 6.67 (1H, t, $J = 7.7$ Hz), 5.80 (1H, s), 3.98 (2H, m), 3.86 (6H, s), 3.83 (3H, s), 2.42 (2H, m). ^{13}C NMR (75 MHz, $CDCl_3$): δ 167.9, 165.9, 153.0 (2C), 143.6, 140.6,139.9, 138.4, 137.9, 132.9, 132.5, 130.0, 127.7, 127.6, 127.2, 125.7, 125.5, 125.2, 124.2, 120.5, 105.3 (2C), 71.5, 60.2, 55.6 (2C), 41.1, 24.1; ESI-MS: *m/z* 496 $[M + Na]^+$; HR-ESI-MS: *m/z* 496.1730 $[M + Na]^+$ (calcd for $C_{28}H_{27}NO_6Na$, 496.1736).

*6.1.9 (E)-3-(Hydroxy(p-tolyl)methyl)-1-(3-(3,4,5-trimethoxyphenyl)acryloyl)-5,6-dihydropyridin-2(1H)-one (**2i**)*

Yield 62%; pale yellow oil; ^{1}H NMR (300 MHz, $CDCl_3$): δ 7.61–7.55 (1H, d, $J = 15.4$ Hz), 7.32 (1H, d, $J = 15.4$ Hz), 7.24 (2H, d, $J = 7.9$ Hz), 7.11 (2H, d, $J = 7.9$ Hz), 6.75 (2H, s), 6.66 (1H, t, $J = 7.6$ Hz), 5.59 (1H, s), 3.99 (2H, m), 3.89 (6H, s), 3.84 (3H, s), 2.45 (2H, m).^{13}C NMR (75 MHz, $CDCl_3$): δ 168.8, 166.7, 153.8 (2C), 144.4, 141.1,140.7, 139.9, 138.8, 137.5, 130.9, 129.4 (2C), 127.0 (2C), 121.4, 106.1 (2C),72.3, 61.3, 56.5 (2C), 42.0, 24.9, 21.6; HR-ESI-MS: *m/z* 460.1732 $[M + Na]^+$ (calcd for $C_{25}H_{27}NO_6Na$, 460.1730).

*6.1.10 (E)-3-(Hydroxy(phenyl)methyl)-1-(3-(3,4,5-trimethoxyphenyl)acryloyl)-5,6-dihydropyridin-2(1H)-one (**2j**)*

Yield 56%; pale brown solid, mp: 137°C; ^{1}H NMR (300 MHz, $CDCl_3$): δ 7.59 (1H, d, $J = 15.4$ Hz), 7.36–7.20 (6H, m), 6.73 (2H, s), 6.67 (1H, t, $J = 7.3$ Hz), 5.62 (1H, s), 3.94 (2H, m), 3.89 (6H, s), 3.83 (3H, s), 2.45 (2H, m). ^{13}C NMR (75 MHz, $CDCl_3$): δ 168.3, 166.2, 153.3 (2C), 143.9, 141.4, 140.8, 140.2, 138.3, 130.4, 128.2 (2C), 127.1, 126.6 (2C), 120.9, 105.6 (2C), 71.8, 60.6, 56.0 (2C), 41.5, 24.4; ESI-MS: *m/z* 423 $[M]^+$; HR-MS (ESI): *m/z* 446.1563 $[M + Na]^+$ (calcd for $C_{24}H_{25}NO_6Na$, 446.1574).

Acknowledgements

The authors gratefully acknowledge keen interest of Dr J. S. Yadav, Director, IICT, Hyderabad, India. RSCK and BP thank CSIR, New Delhi for financial support.

References

[1] D.S. Shewach, *Chem. Rev.* **109**, 2859 (2009).
[2] D.J. Newman, G.M. Cragg, and K.M. Snader, *J. Nat. Prod.* **66**, 1022 (2003).
[3] G.M. Cragg, P.G. Grothaus, and D.J. Newman, *Chem. Rev.* **109**, 3012 (2009).
[4] A.S. Sreedhar and P. Csermely, *Pharmacol. Ther.* **101**, 227 (2004).
[5] P.M. Pechan, *FEBS Lett.* **280**, 1 (1991).
[6] J.A. McCubrey, L.S. Steelman, S.L. Abrams, J.T. Lee, F. Chang, F.E. Bertrand, P.M. Navolanic, D.M. Terrian, R.A. Franklin, A.B. D'Assoro, J.L. Salisbury, M.C. Mazzarino, F. Stivala, and M. Libra, *Adv. Enzyme Regul.* **46**, 249 (2006).
[7] D.G. Lloyd, G. Golfis, A.J. Knox, D. Fayne, M.J. Meegan, and T.I. Oprea, *Drug Discovery Today* **11**, 149 (2006).
[8] F.E. Koehn and G.T. Carter, *Nat. Rev. Drug Discovery.* **4**, 206 (2005).
[9] V.S. Parmar, M.E. Bracke, J. Philippe, J. Wengel, S.C. Jain, C.E. Olsen, K.S. Bisht, N.K. Sharma, A. Courtens, S.K. Sharma, K. Vennekens, V. Van Marck, S.K. Singh, N. Kumar, A. Kumar, S. Malhotra, R. Kumar, V.K. Rajwanshi, R. Jain, and M.M. Mareel, *Bioorg. Med. Chem.* **5**, 1609 (1997).
[10] J.W. Lampe, *Am J Clin Nutr* **78**, 579S (2003).
[11] I.L. Tsai, F.P. Lee, C.C. Wu, C.Y. Duh, T. Ishikawa, J.J. Chen, Y.C. Chen, H. Seki, and I.S. Chen, *Planta Med.* **71**, 535 (2005).
[12] V.R.S. Rao, G. Suresh, K.S. Babu, S.S.N. Raju, M.V.P.S. Vishnu Vardhan, S. Ramakrishna, and J.M. Rao, *Tetrahedron* **67**, 1885 (2011).
[13] D. Jyothi, P. Vanathi, P.M. Gowri, V.R.S. Rao, J.M. Rao, and A.S. Sreedhar, *Toxicol. In Vitro* **23**, 1085 (2009).
[14] A. Seghal, *Curr. Med. Chem.* **10**, 749 (2003).
[15] M. Michaelis, J. Bliss, S.C. Arnold, N. Hinsch, F. Rothweiler, H.E. Deubzer, O. Witt, K. Langer, H.W. Doerr, W.S. Wels, and J. Cinatle, *Clin. Cancer Res.* **14**, 6531 (2008).
[16] B. Maurer-Schultze, M. Siebert, and I.D. Bassukas, *Exp. Cell Res* **174**, 230 (1988).
[17] M.M. Romsdahl, *Exp. Cell Res.* **50**, 463 (1968).
[18] A.S. Sreedhar, C. Soti, and P. Csermely, *Biochim. Biophys. Acta* **1697**, 233 (2004).
[19] M.E. Noble, J.A. Endicott, and L.N. Johnson, *Science* **303**, 1800 (2004).
[20] R.H. Gunby, E. Sala, C.J. Tartari, M. Puttini, C. Gambacorti-Passerini, and L. Mologni, *Anticancer Agents Med. Chem.* **7**, 594 (2007).
[21] R.A. MacCorkle and T.H. Tan, *Cell Biochem. Biophys.* **43**, 451 (2005).
[22] K.M. Pumiglia and S.J. Decker, *Proc. Natl. Acad. Sci. USA* **94**, 448 (1997).
[23] M. Doree and S. Galas, *FASEB J.* **8**, 1114 (1994).